

# Improvement of brain perfusion SPET using iterative reconstruction with scatter and non-uniform attenuation correction

Tomi Kauppinen<sup>1</sup>, Matti O. Koskinen<sup>2</sup>, Sakari Alenius<sup>3</sup>, Esko Vanninen<sup>1</sup>, Jyrki T. Kuikka<sup>1</sup>

<sup>1</sup> Department of Clinical Physiology and Nuclear Medicine, Kuopio University Hospital, and University of Kuopio, Kuopio, Finland

<sup>2</sup> Department of Clinical Physiology and Nuclear Medicine, Tampere University Hospital, Tampere, Finland

<sup>3</sup> Signal Processing Laboratory, Tampere University of Technology, Tampere, Finland

Received 8 January and in revised form 18 April 2000 / Published online: 9 June 2000

© Springer-Verlag 2000

**Abstract.** Filtered back-projection (FBP) is generally used as the reconstruction method for single-photon emission tomography although it produces noisy images with apparent streak artefacts. It is possible to improve the image quality by using an algorithm with iterative correction steps. The iterative reconstruction technique also has an additional benefit in that computation of attenuation correction can be included in the process. A commonly used iterative method, maximum-likelihood expectation maximisation (ML-EM), can be accelerated using ordered subsets (OS-EM). We have applied to the OS-EM algorithm a Bayesian one-step late correction method utilising median root prior (MRP). Methodological comparison was performed by means of measurements obtained with a brain perfusion phantom and using patient data. The aim of this work was to quantitate the accuracy of iterative reconstruction with scatter and non-uniform attenuation corrections and post-filtering in SPET brain perfusion imaging. SPET imaging was performed using a triple-head gamma camera with fan-beam collimators. Transmission and emission scans were acquired simultaneously. The brain phantom used was a high-resolution three-dimensional anthropomorphic JB003 phantom. Patient studies were performed in ten chronic pain syndrome patients. The images were reconstructed using conventional FBP and iterative OS-EM and MRP techniques including scatter and non-uniform attenuation corrections. Iterative reconstructions were individually post-filtered. The quantitative results obtained with the brain perfusion phantom were compared with the known actual contrast ratios. The calculated difference from the true values was largest with the FBP method; iteratively reconstructed images proved closer to the reality. Similar findings were obtained in the patient studies. The plain OS-EM method improved the contrast

whereas in the case of the MRP technique the improvement in contrast was not so evident with post-filtering.

**Key words:** Brain perfusion – Iterative reconstruction – Non-uniform attenuation correction – Single-photon emission tomography

**Eur J Nucl Med (2000) 27:1380–1386**

DOI 10.1007/s002590000291

## Introduction

The conventional, and still the most extensively used, reconstruction technique for single-photon emission tomography (SPET) imaging is filtered back-projection (FBP) [1, 2, 3, 4]. This popularity is attributable to the short computation times, but the technique produces unwanted streak artefacts and has the further disadvantage that the final result is an approximation, and therefore not very accurate. The result is better if a set of corrective steps is performed iteratively during the reconstruction. In this context iteration is a repeated computation process during which the algorithm calculates all the projection data a number of times. The iterations continue until errors reach a prescribed limit or the maximum number of iteration steps is reached [5]. There are many different iterative algorithms for SPET reconstruction depending on how the correction step is performed.

The maximum-likelihood expectation maximisation (ML-EM) algorithm [6, 7] has proved an effective reconstruction technique in SPET imaging, but is unfortunately too slow in clinical use. The most widely used accelerating technique is the ordered subsets (OS) algorithm. It was introduced by Hudson and Larkin in 1994 and was added to the EM algorithm, yielding the ordered subsets expectation maximization (OS-EM) algorithm [8].

*Correspondence to:* T. Kauppinen, Department of Clinical Physiology and Nuclear Medicine, Kuopio University Hospital, P.O. Box 1777, 70211 Kuopio, Finland

The overall accuracy is better when many iterative computation steps are performed, but random noise is increasing in repetitive computations. Some kind of noise reduction method is therefore always needed. A new type of reconstruction algorithm, called median root prior (MRP), is designed especially for noise reduction. This method is not sensitive to the number of iterations [9]. When a new value for a pixel is computed, the prior computes a penalty factor that is applied together with the data-fitting ML-EM coefficient. Certain kinds of images are penalised less than other images. MRP favours images consisting of small neighbourhoods of locally monotonic regions of radioactivity concentrations. This applies well to emission images in general. During the iteration, any deviation of the current pixel value from the median of the pixels in the neighbourhood is penalised. The spatial size of the preserved detail can be adjusted beforehand by the neighbourhood size. The algorithm is called MRP, because a signal that passes the median filter unaltered is a root signal of the median filter [10]. The OS accelerating procedure can also be applied to the MRP algorithm [11].

Quantitative brain SPET imaging has been shown to require scatter and attenuation correction as well as partial volume correction [12]. Scatter correction can be performed iteratively using transmission data [13], where the scatter component is estimated from the photopeak projection data followed by calculation of the convolution of the scatter function [14, 15]. Non-uniform attenuation correction has been shown to be more accurate than uniform attenuating medium approximation [16]. Not only attenuation but also scatter correction can be performed after simultaneous transmission and emission acquisition. Iterative reconstruction algorithms permit use of these corrections during the image reconstruction process. For quantitative purposes, the recovery coefficients can be measured and an appropriate partial volume correction subsequently performed [12].

The aim of this study was to evaluate critically the quantitative accuracy of iterative reconstruction with scatter and non-uniform attenuation correction in SPET brain perfusion imaging. Assessment of the accuracy of the reconstruction methods was performed by comparing organ-like phantom measurements with actual activity values, and also by means of patient perfusion studies. Whereas the reality of the phantom is known, enabling validation, in the patient studies the reality is unknown and these studies consequently represent characterisation of the methods used.

## Materials and methods

*Phantom study.* The phantom used was a high-resolution three-dimensional anthropomorphic JB003 phantom (Nuclemed N.V./S.A., Roeselare, Belgium). This brain phantom is composed of 40 3-mm-thick round polycarbonate plates, which are arranged in a stacked cylinder. The brain structure is mimicked by carving cavi-

ties into the plastic plates. For the grey matter, the entire thickness of plate is cut away, whereas for the white matter only a quarter of it is removed. This yields a grey-to-white matter ratio of 4:1, as advised by the manufacturer. These plates form an anatomical representation of the human brain, each plate corresponding to a transaxial slice. The size of the brain phantom is 120×122×168 mm and its volume is 705 ml when filled with radioactive water. In this study the phantom was used to simulate a "normal" brain. The phantom was filled with 300 MBq of technetium-99m solution and 39 Mcounts (approximately 10 times the patient study) were acquired from SPET acquisition.

*Patient studies and radiopharmaceutical.* The patient studies were performed on ten patients with chronic pain syndromes, such as fibromyalgia and chronic low back pain. The patients were a subgroup of a larger clinical trial approved by the Ethics Committee of Kuopio University Hospital, and participated in the study after giving informed oral consent. The patient group consisted of eight female and two male patients with a mean age of 44 years (range 36–51). The brain perfusion studies were done using <sup>99m</sup>Tc-ethyl cysteinate dimer (ECD) as the tracer (<sup>99m</sup>Tc-NeuroLite, DuPont Pharma, Hertfordshire, UK). The acquired count statistics in each patient varied but on average 3.5 Mcounts were acquired (range 2.0–4.3 Mcounts). The patient dose was 500–600 MBq of <sup>99m</sup>Tc-ECD and in the line source, 550–700 MBq.

*SPET imaging.* Image acquisition was carried out with a Siemens MultiSPECT3 triple-headed gamma camera with fan-beam collimators (Siemens Medical Systems, Inc., Hoffman Estates, Ill., USA). The fan-beam focus of the collimator was 545 mm and the radius of rotation was 180 mm. SPET acquisitions were performed using a 360° orbit for each detector. Transmission and emission scans were acquired simultaneously using one detector, with two detectors being used only for emission scans. For the transmission acquisition, the narrow line source was placed on the focus line of the fan-beam collimator and the object was positioned at the centre of the rotation. The line source for the transmission scan was a 20-cm-long glass tube, with an inner diameter of 4 mm and an outer diameter of 6 mm [17].

A symmetrical 15% wide energy window for the acquisition was centred at 140 keV. SPET imaging was carried out with a 128×128 matrix size using 90 projection angles. The phantom studies were acquired at 75 s per projection angle, and patient studies at 30 s per view. Both transmission and emission acquisitions and blank scan were measured using the same matrix size, radionuclide (<sup>99m</sup>Tc) and acquisition time. Transmission and emission scans were acquired simultaneously, and after acquisition the emission part was subtracted from the transmission data set [17].

*MR imaging.* The brain phantom was also scanned using a 1.5-T magnetic resonance (MR) scanner (Siemens Vision 1.5 T, Erlangen, Germany) and MP-RAGE sequence (T1-weighted sequence, TR 9.7 ms, TE 4.0 ms and flip angle 12°). The phantom was filled with water, containing 38 mg MnCl<sub>2</sub>. By using MR images the reconstructed SPET images and calculated contrast (grey-to-white) ratios can be compared with the absolute values. Hence MR images are a good reference for the contrast ratio calculations, representing another imaging modality that permits measurement of the anatomical distribution of the volume.

*Image processing.* The gamma camera was connected to a Siemens ICON acquisition computer (Siemens Medical Systems, Inc., Hoffman Estates, Ill., USA). The data were transferred to a HERMES software system (Nuclear Diagnostics AB, Hågersten, Sweden). It-

erative reconstruction programs OS-EM (v 5.201) by R. Larkin (Macquarie University, Sydney, Australia) and MRP by S. Alenius (Tampere University of Technology, Tampere, Finland) were installed in the Unix system. Both of them were used simultaneously with the HERMES processing system. The OS-EM and MRP algorithms were used for iterative reconstruction. They demand post-filtering, and the amount of this post-filtering was equalised between FBP and iterative reconstruction. The number of subsets was chosen to be six for the OS-EM algorithm. The number of iterations varied: for the transmission reconstruction four iterations were used, while for the emission reconstruction 12 iterations were used for the phantom and eight iterations for the patient study. The phantom study was reconstructed using more iterations because of higher count statistics. In the MRP calculations 35 iterations were used for transmission and 75 for emission reconstruction. The selected value of the  $\beta$ -parameter (a penalising weighting factor) was 0.3, based on previous experiments [18]. MRP calculates the median in a small local 5×5 mask. A larger 256×256 matrix size was chosen for the gamma images to keep the actual dimensions of the local median mask as small as possible.

The original acquisition file and blank scan were required for the transmission-dependent scatter correction (TDSC). Scatter estimation was based on the point source measurement as previously described [17, 19]. Non-uniform attenuation correction requires patient-specific attenuation maps (AMAPs), which are based on the count ratio between the image-represented transmitted count rate through the subject and the blank scan. AMAPs can be performed in iterative reconstruction programs [16]. Both TDSC and non-uniform attenuation corrections were done after SPET imaging as well as in phantom and patient studies.

FBP images were scatter corrected based on the TDSC technique [19]. Attenuation correction was applied to the reconstructed slices using Chang's first-order approximation, because attenuation correction based on the transmission acquisition is not available in the FBP reconstruction method. The linear attenuation correction was  $\mu=0.12\text{ cm}^{-1}$  for the phantom study and  $\mu=0.10\text{ cm}^{-1}$  for the patient studies. In the FBP technique the projection images were pre-filtered by a Butterworth filter based on the visual impression and quality of slices. The cut-off frequency  $0.6\text{ cm}^{-1}$  and order 6 were selected. In order to achieve a similar visual appearance, iterative reconstruction techniques were used with Butterworth post-filtering. Because filtering techniques are slightly different depending on whether filtering is done before or after reconstruction, the filtering had to be equalised. The filter parameters were set such that the standard deviation (SD) of a uniform region was the same for all methods. A uniform slice of the phantom was used for the filter equalisation and in the case of the patient studies a uniform

brain area (cerebellum) was used. Hence the amount of filtering was optimised independently for each iterative reconstruction technique and was not necessarily identical between different methods. The projection images reconstructed by FBP were filtered first and then the iteratively reconstructed images were filtered. The parameters of the post-filtering were based on the uniformity profile and the standard deviation of the uniform area. When the uniformity profile and SD were set equal between the FBP and the iterative technique, then the amount of post-filtering was accepted.

**Contrast analysis.** Quantitative analysis of the phantom study was based on comparison of the mean count densities in regions of interest (ROIs) in the reconstructed slices. Partial volume correction with the recovery coefficient was not applied. The regional mean count density of grey matter was divided by the comparable white matter value.

ROI drawing was performed using the "MultiModality" analysis program in the HERMES workstation (Nuclear Diagnostics AB, Hägersten, Sweden). For the analysis, three successive slices were summed and ROIs were drawn manually using LT30% cut-off on the OS-EM image and then copied to the FBP or MRP images. The left hemisphere was drawn first and then the mirror images of ROIs were placed on the right hemisphere and positioned correctly. The ROIs were drawn individually for each anatomical location. For the quantitative analysis, 18 different regions were defined in the reconstructed slices and these regions were also arranged into three groups. The regions of the cerebellum, hippocampus and pons were arranged into (1) subtentorial areas, (2) cortical areas encompassing the frontal, occipital and parietal lobes and (3) subcortical areas including the caudate nucleus, putamen and thalamus. In addition, white matter regions were drawn above the ventricle level over a large common area for the ratio calculation.

The human studies were analysed in the same way as the brain perfusion phantom studies, but because in human studies the true activity concentration and distribution are unknown, the results were compared between different reconstruction algorithms. The statistical calculations were carried out using the non-parametric Wilcoxon signed-ranks test.

## Results

### The brain phantom

The analysis of the brain phantom data was carried out by calculating the grey-to-white matter ratio in all 18 regions and in the three subgroups. Then the regional re-

**Table 1.** Results of the regional analysis of the brain phantom, where each brain region (mean counts) is adjusted by mean counts of the white matter region

	Actual	MRI	FBP		OS-EM		MRP	
			Mean±SD	$\Delta\%\pm\text{SD}$	Mean±SD	$\Delta\%\pm\text{SD}$	Mean±SD	$\Delta\%\pm\text{SD}$
Subtentorial areas	4.0	2.8±0.5	2.4±0.2	12.3±9.3	2.7±0.3	1.7±8.4	2.5±0.1	8.1±11.3
Cortical areas	4.0	3.3±0.1	2.6±0.2	21.5±7.4	2.8±0.2	15.3±7.4	2.8±0.1	15.6±3.2
Subcortical areas	4.0	3.4±0.2	2.8±0.2	18.0±9.7	3.0±0.3	13.6±8.9	2.7±0.4	22.2±10.9
All regions	4.0	3.2±0.4	2.6±0.3	17.9±9.0	2.8±0.3	11.3±9.6	2.7±0.2	16.2±10.0

Percentage difference ( $\Delta\%$ ) was calculated comparing SPET values with MR values. The total number of regions was 18. Subtentorial areas contained 4 brain regions, cortical areas 6, and subcortical areas 6

sults were compared with the absolute phantom value 4.0 (Table 1). The percentage differences between contrast ratios and the actual values are presented in Fig. 1. Comparison was also made with values calculated using MR images, although actual values are unattainable by MR imaging because summation of slices adversely affects definition of the edge of the phantom owing to its

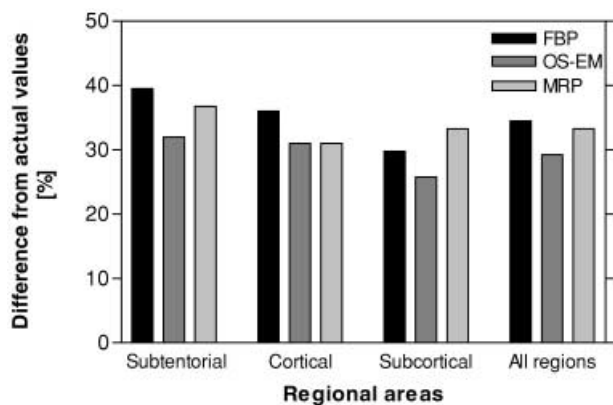


Fig. 1. Percentage differences from the actual contrast values

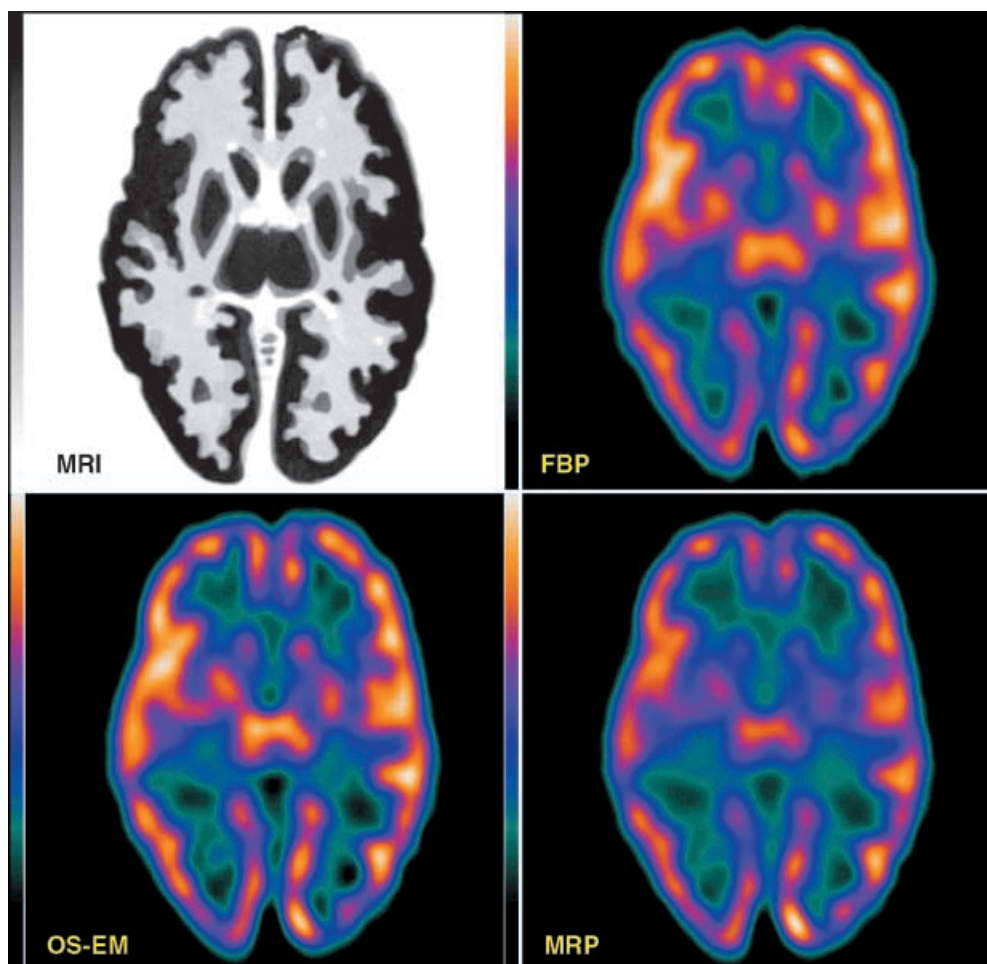
curved surface. The quality of iterative reconstruction is presented in Fig. 2.

Iterative reconstruction increased the contrast of the image and improved separation between the different regions. The calculated differences from the actual values were largest with the FBP method, except in the subcortical areas, where they were largest with MRP. In all the regions, the percentage mean differences from the actual values were 35% with FBP, 29% with OS-EM and 33% with MRP. Iterative OS-EM reconstruction increased the contrast of the image and improved separation between the different regions. The improvement compared with FBP was approximately 8% in OS-EM in all regions and 2%–4% when using the MRP reconstruction method.

#### Patient studies

The quality of the reconstructed images was judged using the regional grey-to-white matter ratio, acquiring transmission and emission data simultaneously. The calculated values were subgrouped (Fig. 3), as in the case of the phantom study. There was a statistically signifi-

Fig. 2. The middle slice of the brain phantom reconstructed by FBP, OS-EM and MRP reconstruction methods. The MR image is taken from the same level as SPET images. Three successive slices were summed and equalised filtering was used on the different reconstruction techniques. OS-EM images were computed using 12 iterations with six ordered subsets, whereas MRP images were reconstructed using 75 iterations. For the FBP reconstruction a Butterworth filter with cut-off frequency  $0.6 \text{ cm}^{-1}$  was selected. Colour scale is Warm Metal; LT=0% and UT=100%



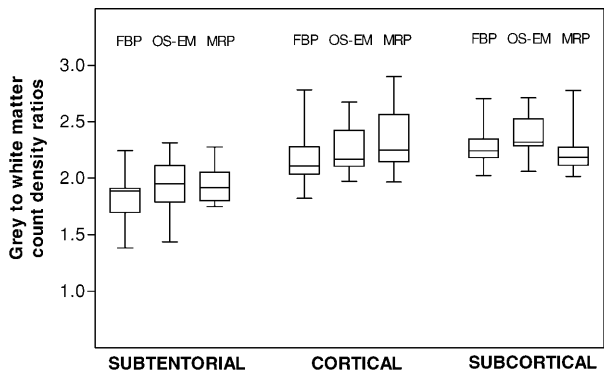
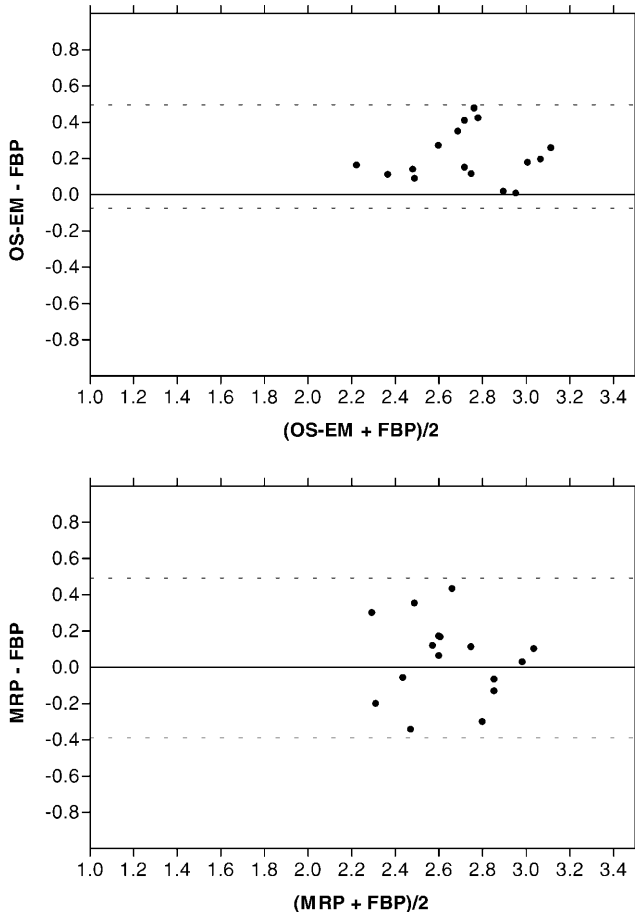


**Fig. 3.** The count density ratios of perfusion study subjects ( $n=10$ ) calculated by different reconstruction techniques and presented in the brain area subgroups (see text for further details). Half of all the observations are in the boxes. The median of the ratio is shown as a line in the boxes and the range is also indicated

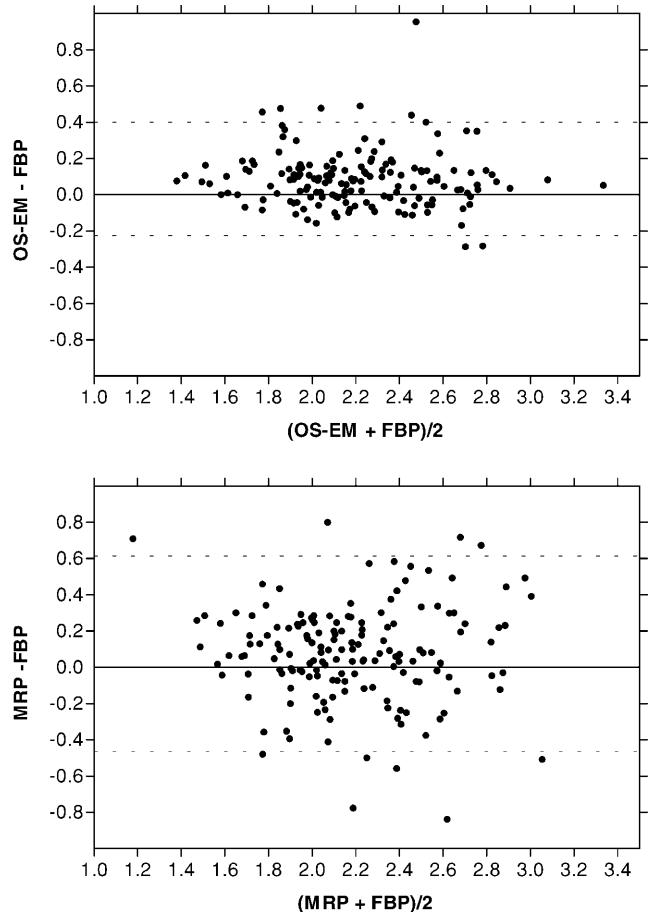
**Fig. 4.** Differences between grey-to-white count density ratios obtained by iterative reconstruction and FBP plotted against the average. Limits of agreement (95% range) are shown by *dotted lines*. The *left image pair* presents limits of agreements in the brain perfusion phantom study, and the *right image pair* shows the contrast ratios between grey and white matter in each region for each patient. The *upper images* compare calculations for OS-EM versus FBP, and the *lower images*, calculations for MRP versus FBP



cant difference in most of the OS-EM versus FBP calculations, while the difference in the MRP versus FBP calculations was significant only in cortical areas. The statistical significance of differences between the reconstruction techniques with respect to the various areas is indicated in Table 2. The data can be analysed using limits of agreement presentations (Fig. 4). Comparison of OS-EM and FBP results revealed that limits of agreement were 0.31 for OS-EM and 0.54 for the MRP, when all regions of each patient were compared. For the phantom study these values were 0.29 for OS-EM and 0.44 for MRP. The correlation coefficients were  $r=0.87$  and  $r=0.83$ , respectively. Figure 4 demonstrates that OS-EM improves contrast whereas the quantitative improvement achieved by the MRP technique is not significant.

**Table 2.** Statistical significance between results of different reconstruction techniques. Wilcoxon signed-ranks test was used in each subgroup

Area	<i>P</i> value: OS-EM vs FBP	<i>P</i> value: MRP vs FBP
Subtentorial areas	0.059	0.059
Cortical areas	0.037	0.007
Subcortical areas	0.017	0.445
All regions	0.017	0.169



## Discussion

Since the late 1970s the advantages of iterative reconstruction methods have been discussed in the literature. Several iterative reconstruction methods have been published and proposed for use in SPET reconstruction, but few of them have been applied in the clinical environment. Only a few comparisons of different reconstruction methods have been published [20, 21]. In this work, two different types of iterative reconstruction method were evaluated and the results compared with the results obtained using the FBP technique. Iterative reconstruction algorithms have been demonstrated to produce qualitatively accurate images and they allow incorporation of simultaneous attenuation and scatter corrections for image-degrading effects during reconstruction.

Computation time is an important factor in the reconstruction process. For the reconstruction to be feasible in the clinical environment, computation times have to be reasonable. Traditionally FBP reconstruction takes only a few minutes, whereas iterative reconstruction typically requires much longer. However, the latest iterative techniques, especially those with an accelerating procedure (e.g. OS-EM), have achieved reasonable computation times [8, 11, 22].

As discussed earlier, not only scatter and attenuation corrections but also iterative reconstruction and partial volume correction are necessary for quantitative SPET imaging. Different correction techniques have been proposed for photon attenuation correction, but the most accurate techniques are based on the actual density distribution of the object. In this study, the transmission scan was measured simultaneously with the emission scan, which offers many obvious advantages, including the fact that the patient position is exactly the same. AMAPs were reconstructed separately using OS-EM and MRP techniques and used for the non-uniform attenuation correction. Scatter correction and attenuation correction techniques have been investigated widely, and various correction techniques have been proposed. TDSC was published by Meikle et al. [13] and Bailey and Meikle [15] and for this study it was used in the way presented in the papers of Yang et al. [17, 19]. Attenuation and scatter corrections can be carried out using the same AMAP information with optimal measurement and computation time. The comparison between reconstruction methods was made with uniformity-matched filtering. Partial volume correction was not applied in this study because the aim of the study was to compare the three reconstruction techniques.

The quantitative results obtained with the perfusion phantom were compared with the actual results using regional analysis. As already mentioned, because the reality of the phantom is known, the phantom study enables validation, whereas in the patient studies the reality is unknown. Thus, the patient studies represent characterisation of the methods used. The FBP method yielded re-

sults which were the farthest from the actual contrast ratios, whereas the results obtained using OS-EM were the nearest to reality. With the OS-EM algorithm, the improvement was similar in different regions, whereas the MRP algorithm improved the results markedly in the subtentorial and cortical areas but only slightly in the subcortical areas. The improvement achieved by the MRP method with post-filtering is not so evident in emission reconstructions, but MRP has a clear advantage in the attenuation map reconstruction because it uses the median of the data signal and also because it acts monotonously. The MRP method can be improved if additional options, such as increase in the matrix or median mask size, are included in the calculation.

MR reference images were acquired because they represent the anatomical distribution of the volume. It was noticed that absolute contrast values, given by the manufacturer, are unattainable even with the MR technique, although MR images are closer to the real values than contrast values calculated by SPET.

The quality of the patient data was judged using the same regional analysis as in the perfusion phantom study, but in the case of the patient studies the reality was not known and there was not a golden standard with which to compare the results. Hence the calculated results had to be compared with each other. The improvement with the OS-EM method behaved in a straightforward manner, but with the MRP technique the contrast in the subcortical areas was worse than with the FBP technique. A similar finding was found in the brain phantom measurements. There were statistically significant differences between the results of the reconstruction methods in different subgroups, and also in all regions when comparing the results of OS-EM and FBP. The results reconstructed using the MRP algorithm were accurate and statistically significant in subtentorial and cortical areas, but not in subcortical areas.

The FBP reconstruction method gives the first approximation of activity distribution. The result is therefore noisy and includes harmful streak artefacts. All this has been known ever since the technique was first employed, but to date the FBP algorithm has been the only choice because of the computing time needed for iterative processes. The speed of the reconstruction process is no longer a problem when using accelerated computation algorithms and modern computers. Iterative reconstruction algorithms improve the results of SPET brain perfusion imaging, especially when the correct number of iterations and proper filtering are selected. Iterative reconstruction algorithms (OS-EM) are recommended for brain SPET reconstruction in clinical situations.

*Acknowledgements.* This work was financially supported by Kuopio University Hospital (EVO funding); this support is gratefully acknowledged, as are the help and support of Nuclear Diagnostics Ltd. (Hägersten, Sweden). The authors want to express sincere thanks to Jiwei Yang, PhD, for his technical support of TDSC and to Mervi Könönen, MSc, for her kind help with MR imaging.

## References

1. Brooks RA, Di Chiro G. Principles of computer assisted tomography (CAT) in radiographic and radioisotopic imaging. *Phys Med Biol* 1976; 21: 689–732.
2. Larsson SA. Gamma camera emission tomography: development and properties of a multi-sectional emission computed tomography system. *Acta Radiol* 1980; 363: 1–75.
3. Bracewell RN, Riddle AC. Inversion of fan-beam scans in radio astronomy. *Astrophys J* 1967; 150: 427–434.
4. Ramachandran GN, Lakshminarayanan AV. Three-dimensional reconstruction from radiographs and electron micrographs: application of convolutions instead of Fourier transforms. *Proc Nat Acad Sci USA* 1971; 68: 2236–2240.
5. Rusinek H. SPECT reconstruction techniques. In: Kramer EL, Sanger JJ, eds. *Clinical SPECT imaging*. New York: Raven Press; 1995: 43–67.
6. Shepp LA, Vardi Y. Maximum likelihood reconstruction for emission tomography. *IEEE Trans Med Imaging* 1982; MI-1: 113–122.
7. Lange K, Carson R. EM reconstruction algorithms for emission and transmission tomography. *J Comput Assist Tomogr* 1984; 8: 306–316.
8. Hudson HM, Larkin RS. Accelerated image reconstruction using ordered subsets of projection data. *IEEE Trans Med Imaging* 1994; 13: 601–609.
9. Alenius S, Ruotsalainen U. Bayesian image reconstruction for emission tomography based on median root prior. *Eur J Nucl Med* 1997; 24: 258–265.
10. Alenius S, Ruotsalainen U, Astola J. Using local median as the location of the prior distribution in iterative emission tomography image reconstruction. *IEEE Trans Nucl Sci* 1998; 45: 3097–3104.
11. Seret A. Median root prior and ordered subsets in Bayesian image reconstruction of single-photon emission tomography. *Eur J Nucl Med* 1998; 25: 215–219.
12. Almeida P, Ribeiro MJ, Bottlaender M, Loc'h C, Langer O, Strul D, Hugonnard P, Grangeat P, Mazière B, Bendriem B. Absolute quantitation of iodine-123 epidepride kinetics using single-photon emission tomography: comparison with carbon-11 epidepride and positron emission tomography. *Eur J Nucl Med* 1999; 26: 1580–1588.
13. Meikle SR, Hutton BF, Bailey DL. A transmission-dependent method for scatter correction in SPECT. *J Nucl Med* 1994; 35: 360–367.
14. Axelsson B, Msaki P, Israelsson A. Subtraction of Compton-scattered photons in single-photon emission tomography. *J Nucl Med* 1984; 25: 490–494.
15. Bailey DL, Meikle SR. A convolution-subtraction scatter correction method for 3D PET. *Phys Med Biol* 1994; 39: 411–424.
16. Bailey DL. Transmission scanning in emission tomography. *Eur J Nucl Med* 1998; 25: 774–787.
17. Yang J, Kuikka JT, Jaatinen K, Länsimies E, Patomäki L. A novel method of scatter correction using a single isotope for simultaneous emission and transmission data. *Nucl Med Commun* 1997; 18: 1071–1076.
18. Kauppinen T, Alenius S, Turjanmaa V, Kuikka J, Koskinen M. Comparison between iterative median root prior algorithm and filtered back-projection in SPET [abstract]. *Eur J Nucl Med* 1998; 25: 948.
19. Yang J, Kuikka JT, Vanninen E, Kauppinen T, Länsimies E, Patomäki L. Evaluation of scatter correction using a single isotope for simultaneous emission and transmission data. *Nuklearmedizin* 1999; 38: 49–55.
20. Llacer J, Veklerov E, Baxter LR, et al. Results of a clinical receiver operating characteristic study comparing filtered back-projection and maximum likelihood estimator images in FDG PET studies. *J Nucl Med* 1993; 34: 1198–1203.
21. Hutton BF, Hudson HM, Beekman FJ. A clinical perspective of accelerated statistical reconstruction. *Eur J Nucl Med* 1997; 24: 797–808.
22. Byrne CL. Accelerating the EMLL algorithm and related iterative algorithms by rescaled block-iterative methods. *IEEE Trans Image Processing* 1998; 7: 100–109.